Int J Adv Manuf Technol (2009) 41:226–233
DOI 10.1007/s00170-008-1478-5

ORIGINAL ARTICLE

Optimal design of electrode cooling system for resistance spot welding with the response surface method

X. M. Lai · A. H. Luo · Y. S. Zhang · G. L. Chen

Received: 27 July 2007 / Accepted: 10 March 2008 / Published online: 16 April 2008

Abstract Resistance spot welding (RSW) is typically used in automobile body assembly, where continuous efficiency depends on electrode life, which is closely related with the water cooling effect. In this paper, the finite element simulation and response surface analysis methods are adopted to optimize the RSW electrode cooling process. Aiming to optimal cooling parameters and improve cool effect, we present a special sphere-shape weld cap with inlet pipe and cooling cavity and model its cooling effect as non-linear polynomial equations, which can avoid numerous influential factors. Electrode parameters, including pipe diameter, pipe height and flow velocity, are adjusted according to these non-linear equations. Optimization is carried out subsequently and experimental measurements on electrode diameters are performed for validation. It is found that the response surface model not only indicates the direction of design modification, but also leads to an optimal method for electrode design.

Keywords Optimal design · Response surface · Spot welding electrode

1 Introduction

Resistance spot welding (RSW) is extensively used in automotive industry due to its relatively low capital, operating costs and its potential for high production rates. It is accomplished by making an electrical current pass through upper electrode, workpieces and lower electrode in turn. Due to contact resistance between workpieces, Joule heat obtained from the interface causes the mating workpieces to fuse together. With the application of new materials, especially galvanized steels, electrode wear and thermal degradation have become more and more serious and many studies have been done in recent years [1–4]. In the RSW processes, redundant heat is taken away by water which continually flows over the cooling channel at the end of electrode. Efficient transfer of heat from the electrode to the water can reduce the electrode temperature and limit thermal degradation of the electrode material. A proper electrode temperature results in longer electrode life and higher spot welding efficiency. However, electrode temperature is usually affected by various electrode design and process parameters, such as electrode shape, internal water cooling tube position, cooling water flow rates, and electrode face thickness.

Much experimental research on electrode cooling water has been carried out to study the effects of water flow rate and water temperature [5–7]. Both of which have important impact on electrode cooling, while the latter is more important than former on electrode life [7]. However, electrode cooling efficiency increases rapidly with higher flow rates before its effect on cooling becomes saturated [6–9]. After the cooling effect is saturated, it changes rapidly under low water velocity and in small pipe diameter, while varying little under high water velocity and in large pipe diameter. The effectiveness of water flow rate on electrode cooling depends on the size of the water cooling tube. A stagnant boundary water layer or boiling of the water in the cooling tube can reduce electrode life [5, 10]. For a given geometry, heat dissipation from electrode to water keeps at the same level regardless of flow rate [6].

X. M. Lai (✉) · A. H. Luo · Y. S. Zhang · G. L. Chen
BMTC, School of Mechanical and Power Engineering,
Shanghai Jiao Tong University,
800 Dongchuan Road,
Shanghai, People's Republic of China
e-mail: xmlai@sjtu.edu.cn

With the advances of computer technologies and finite element methods in the past two decades, it is now possible to model many different complex welding processes such as arc welding, friction welding and spot welding. However, probably because of the complexity involved in the modeling of the electrode cooling process, few attempts have been reported in the literature. In 1999, Yeung and Thornton from Ford Motor Company developed a parametric model by using FEM to predict thermal behavior of an electrode cap [11]. But water flow behavior and cooling efficiency with different shape of electrode have not been discussed.

This study uses the CAD software to create an electrode model and finite element software to analyze the conditions of cooling processing. It simulates the temperature distribution of electrode under various parameters (pipe height h, pipe diameter D, water velocity v), as shown in Fig. 1, as well as using response surface method to establish the relationship between cooling rate and cooling system parameters. Based on the RSM modeling technique, one can represent the complicated and uncertain relationships between the input variables and the output ones.

When the response has constructed the relationships of the input and output electrode cooling variables, an appropriate optimization algorithm is able to search for the optimal cooling parameters. In this paper, the GA optimization method is adopted, which is a high efficient search strategy by parallel searching function at multiple points [12].

2 Electrode cooling flow theory and evaluation

2.1 Electrode cooling flow theory

In RSW, high welding current passes through upper electrode, workpieces and lower electrode. Because of the electrical contact resistance and bulk resistance, Joule heat will be generated at the three interfaces and in the bulks of these components (bulk resistance is much less than interface resistance). The heat at the faying face melts the workpieces to form a nugget. The rest of heat enters the electrode and would been taken away by the cooling water, which is circulated in the cooling cavity of the electrode. The governing equations of electrode cooling flow theory are as follows [13]:

1. The continuity equation, analyses the water flowing and different temperature distribution in the cooling process. It has to consider the heat transfer. By mass conservation:

$$\frac{\partial \rho}{\partial t} + \overline{\nabla} \bullet \left(\overrightarrow{\nabla} \overrightarrow{V}\right) = 0 \tag{1}$$

where ρ is material density and V is vector velocity.

2. The momentum equation, Newton's second law, is used to derive the momentum (acceleration condition) or force balance generated by the water flow:

$$\rho\left[\frac{\partial \overrightarrow{V}}{\partial t} + \left(\overrightarrow{V} \bullet \overrightarrow{\nabla}\right)\overrightarrow{V}\right] = -\overrightarrow{\nabla} P + \overrightarrow{\nabla} \bullet \overrightarrow{\overrightarrow{\tau}} + \rho \overrightarrow{f} \tag{2}$$

where P is flow pressure, f is body force and τ represents stress tensor.

3. Energy equation, conservation of the energy of the system; uses the laws of solid/liquid conservation of water flow. If it is the incompressible fluid:

$$\rho C_P\left[\frac{\partial T}{\partial t} + \left(\overrightarrow{V} \bullet \overrightarrow{\nabla}\right)T\right] = -\overrightarrow{\nabla} \bullet q + \overrightarrow{\overrightarrow{\tau}} \cdot \overrightarrow{\nabla} \cdot \overrightarrow{V} \tag{3}$$

where T represents temperature, C_P is specific heat of constant pressure and q is heat flux.

4. Cooling analysis, this is mainly a function of the heat transfer Eq.

$$\rho C_P \frac{\partial T}{\partial t} = k\left[\frac{\partial^2 T}{\partial x_1^2} + \frac{\partial^2 T}{\partial x_2^2} + \frac{\partial^2 T}{\partial x_3^2}\right] \tag{4}$$

The aim of the FEM study was to get a closer look at temperature development in the cooling system for electrode as a function of the cooling process. A FE model for electrode cooling simulation was set up as a 3D model utilizing the FE code Fluent 6.2.16, which is a general-purpose code for analyzing flow, heat transfer and coupled problems.

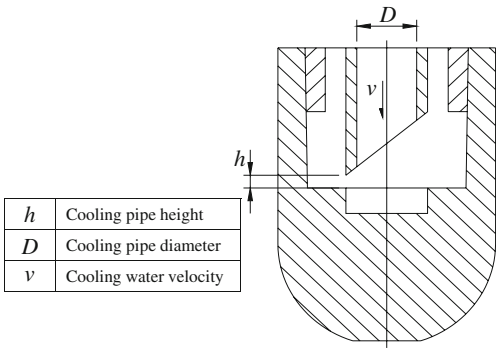

Fig. 1 Relationship between cooling parameters and electrode

2.2 Cooling effect evaluation criterion

In order to determine the cooling effect, cooling rate is defined to be as the evaluation criterion.

$$C_r = \frac{T_{\max}}{T_0} \tag{5}$$

where T_0 is reference temperature, here is 300 K, T_{max} is maximum temperature of the electrode.

3 Response surface modeling and experiment design

3.1 Response surface method

RSM searches for the input combination that optimizes the simulation output. By using the results of a numerical experiment in the points of orthogonal experimental design, response surface analysis is much less computationally expensive than conventional solution using the original method [14].

Generally, the relationship between the response variable of interest and the predictor variables $(x_1, x_2, \cdots x_k)$ may be known exactly as a description:

$$y = g(x_1, x_2, \cdots x_k) + \varepsilon \tag{6}$$

where ε is model error and includes measurement error and other variability.

The experiment approximates the system function $g(x_1, x_2, \cdots x_k)$ with an empirical model of the form:

$$y = f(x_1, x_2, \cdots x_k) + \varepsilon \tag{7}$$

where $f(x_1, x_2, \cdots x_k)$ is the polynomial of order three or less.

The successful application of RSM relies on the identification of a suitable and precise approximation for $f(x_1, x_2, \cdots x_k)$. A second-order could be of the type

$$y = \alpha_0 + \sum_{i=1}^{n} \alpha_i x_i + \sum_{i=1}^{n} \alpha_{ii} x_1^2 + \sum_{p<1}^{n} \alpha_{pi} x_p x_i + \varepsilon \tag{8}$$

The common approach in the RSM is to use regression methods based on least square methods. The method of least square is typically used to estimate the regression coefficient, which is

$$\begin{aligned} \widehat{\alpha} &= [\widehat{\alpha}_0 \widehat{\alpha}_1 \cdots \widehat{\alpha}_n]^T = \left(\mathbf{x}^T \mathbf{x}\right)^{-1} \mathbf{x}^T y \\ &= \left[\frac{1}{k} \sum_{j=1}^{k} y_i, \sum_{j=1}^{k} x_{1j} y_j \Big/ \sum_{j=1}^{k} x_{1j}^2, \cdots, \sum_{j=1}^{k} x_{nj} y_j \Big/ \sum_{j=1}^{k} x_{nj}^2\right]^T \end{aligned} \tag{9}$$

where n is the number of objective function and k is the number of variables.

This is often termed the main effects model since it only includes the main effects of the variables$(x_1, x_2, \cdots x_k)$. The $\widehat{\alpha}$ terms comprise the unknown parameter set which can be estimated by collecting experimental system data. These data can either be sourced from physical experiments or from previously designed dynamic computer models. The parameter set can be estimated by regression analysis based upon the experimental data.

4 Orthogonal experiment design

Cooling effect problem can be described as a response surface by viewing it as an input-output model. As mentioned in Sect. 1, the variables are defined as v, h, D. The values of them are listed in Table 1.

The variables are known as natural variables since they are expressed in physical units of measurement. In the RSM, these variables are transformed into coded variables that are dimensionless, zero mean and the same standard deviation. So, we adopt the transformation on the basis of $x_i = \frac{a_i - (a_{1i} + a_{-1i})/2}{(a_{1i} - a_{-1i})/2}$, where a_{i} is the natural variable. $a_{\text{-1i}}$ and $a_{1\mathrm{i}}$ are the values of the natural variable in level -1 and 1 separately as shown in Table 1.

$$x_1 = \frac{v - 9.25}{5.75},\ x_2 = \frac{h - 4.5}{3.5},\ x_3 = \frac{D - 3.2}{2.2} \tag{10}$$

In this way, the values of parameters are transformed into the code [-1, 1], which represent the original values. Therefore, all the main effects considered in the experiment can be transformed into certain numbers of columns in the design matrix using the above replacement.

In order to simplify the logistic regression to an approximate procedure for checking factor's effects, orthogonal combination DOE method is used to obtain the design matrix. Orthogonal array are utilized to set up fractional designs. After factors are assigned to the columns in an orthogonal array, each row stands for an experimental run in a fractional factorial designs, there is a design matrix corresponding to its design for regression analysis. Orthogonal unitized design matrix includes three types of experiment point.

$$k = m_c + m_r + m_0 \tag{11}$$

Table 1 Values of design variables

Level	$v(m/s)$	$h(mm)$	$D(mm)$
-1	3.5	1	1
1	15	8.0	5.4

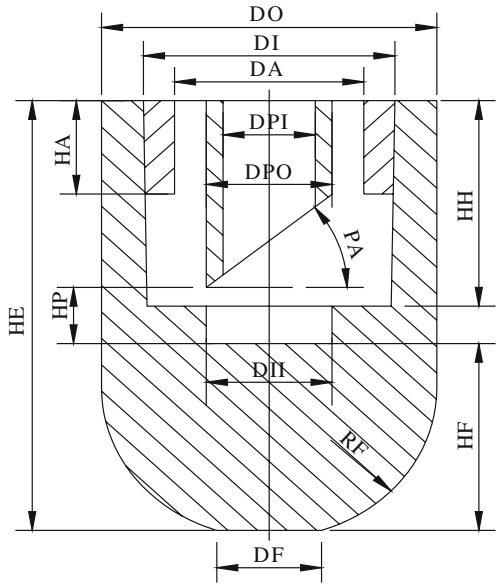

Fig. 2 Schematic diagram of the geometry model

Table 2 Geometry parameters of the simulation model

Parameter	Value(*mm*)	Parameter	Value(*mm*)
DPI	4.4	*HE*	23
DPO	6	*HF*	10
DI	12	*HP*	3
DO	16	*HH*	11
DII	6	*HA*	5
DF	5	*PA*	30°
DA	9	*RF*	16

where $m_c=2^n$ two levels points, m_r=2n star points which have arm length γ, m_0=zero level point. γ can be calculated by the equation:

$$\gamma^2 = \frac{\sqrt{km_c} - m_c}{2} \tag{12}$$

When three factors (n=3) and one zero(m_0=1) point are included in the design, we can get the value of γ^2 from Eq. (12). As to this problem, it has three factors of three levels. The appropriate one for arranging the three factors above with three levels for each is $L_{15}(2^3+2\times3+1)$. Each of (x_1, x_2, x_3) is replaced by three levels, respectively. The orthogonal unitized experiments are arranged as:

$$\mathbf{D} = \begin{bmatrix} x_1 & -1 & -1 & -1 & -1 & 1 & 1 & 1 & 1 & 0 & -\gamma & \gamma & 0 & 0 & 0 & 0 \\ x_2 & -1 & -1 & 1 & 1 & -1 & -1 & 1 & 1 & 0 & 0 & 0 & -\gamma & \gamma & 0 & 0 \\ x_3 & -1 & -1 & -1 & 1 & -1 & 1 & -1 & 1 & 0 & 0 & 0 & 0 & 0 & -\gamma & \gamma \end{bmatrix}^T \tag{13}$$

Note that all these resulting columns are orthogonal in a sense that the inner product of any two of them is equal to zero. No interaction among the three factors is assumed here.

5 Create the relationship between cooling system and cooling rate

5.1 Experiment

Spot welding electrode design involves the design of the inlet pipe, cavity shape, electrode shape, etc. The purpose of this study is to find the optimal cooling system of the spot welding electrode.

Table 3 Material properties

Material properties	Electrode/Tube	Water
Density (kg/m_3)	8800	988.3
Viscosity ($kg/m\cdot s$)	——	0.001
Conductivity ($W/m\cdot K$)	322	0.5996
Specific heat ($J/kg\cdot K$)	390	4182

Table 4 Results of central combination DOE of the cooling effect

No	Factors			Results	
	v	*h*	*D*	T_{max}	c_r
1	3.5	1	1	999.5966	3.331989
2	3.5	1	5.4	789.5467	2.631822
3	3.5	8	1	965.8978	3.219659
4	3.5	8	5.4	887.0880	2.956960
5	15	1	1	806.1325	2.687108
6	15	1	5.4	720.4057	2.401352
7	15	8	1	796.5740	2.655247
8	15	8	5.4	753.5720	2.511907
9	9.25	4.5	3.2	743.1860	2.477287
10	2.27	4.5	3.2	872.7629	2.909210
11	16.24	4.5	3.2	715.8926	2.386309
12	9.25	0.25	3.2	745.8992	2.486331
13	9.25	8.75	3.2	743.1296	2.477099
14	9.25	4.5	0.6	909.7803	3.032601
15	9.25	4.5	5.87	760.6779	2.535593

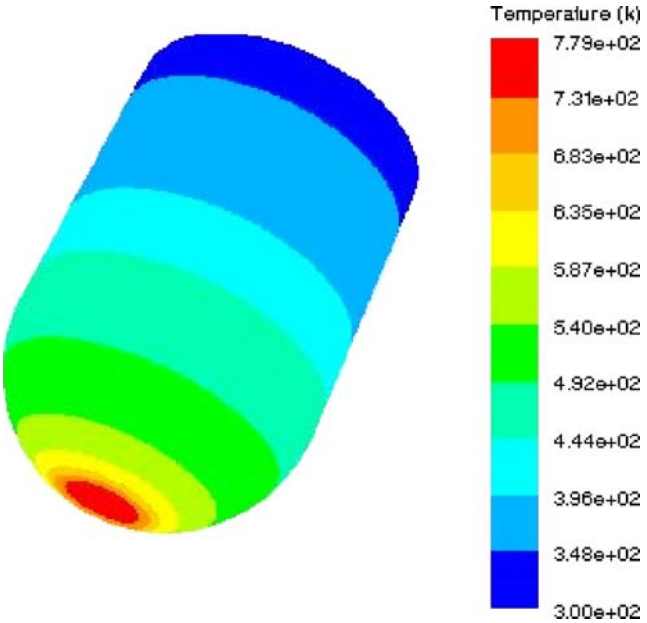

Fig. 3 Contour of temperature on the electrode cap

The sphere weld cap, a common production electrode cap, is chosen for this study. As shown in Fig. 2, the section in blank is the interior of cooling tube and the electrode cooling cavity. The specific values of parameters in this simulation are shown in Table 2. Temperature independent material properties, given in Table 3, are applied to the fluid elements (water in the cooling cavity) and the solid (electrode and water tube).

In the simulations, thermal boundary condition was set on the surface of electrode bottom. The power, dissipated into the electrode, is 910 W approximately [15]. Therefore, heat flux, 5×10^7 W/m^2 is applied on the surface. Because of the direct contact with air, convection and heat radiation have been occurred between the other surfaces of electrode and the air. According to the previous study [11], this part of heat dissipation is much less than the part dissipated into the cooling water. It is about 14 W, 1.78×10^5 W/m^2 two orders of the magnitude relative to the input power. So, this part of heat dissipation is been ignored in this study. At the same time, flow boundary is set on the inlet and outlet. Velocity inlet boundary condition and pressure outlet boundary condition are defined. The initial temperature of the electrode and the inlet temperature of the cooling water is 300 K.

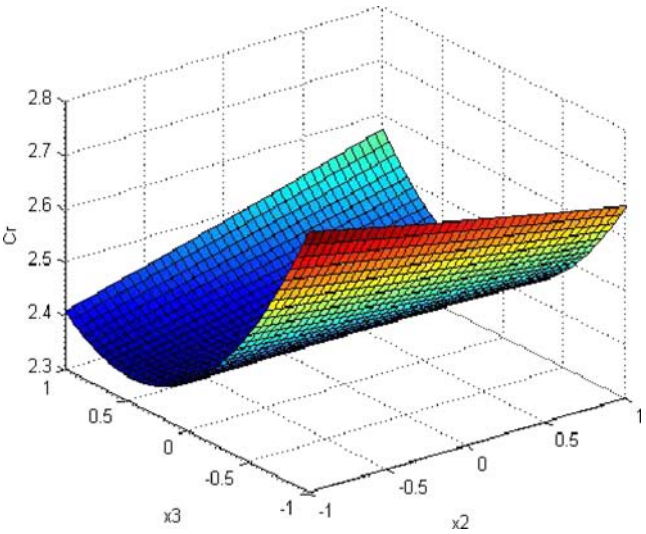

Fig. 5 RSM of cooling rate ($x_1 = 1$)

According to different cooling parameters and orthogonal experiments design, there are 15 sets of data to simulate electrode cooling processing. The experiments and results of simulation are listed in Table 4.

Figure 3 shows the temperature distribution of the electrode, where the maximum value locates at the bottom of the electrode.

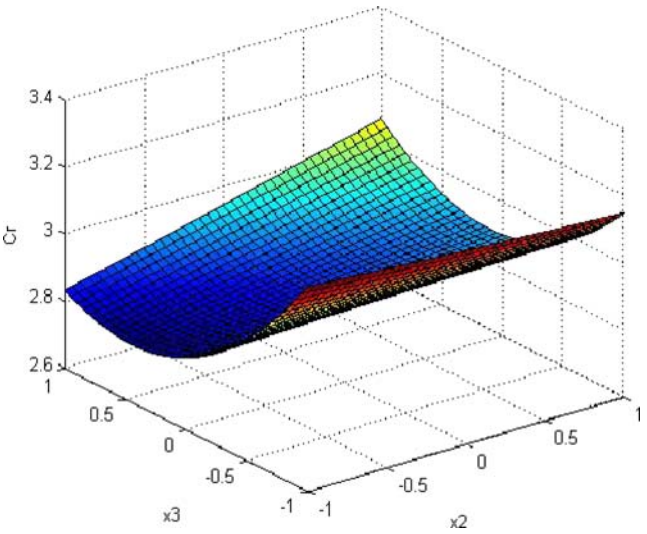

Fig. 4 RSM of cooling rate ($x_1 = -1$)

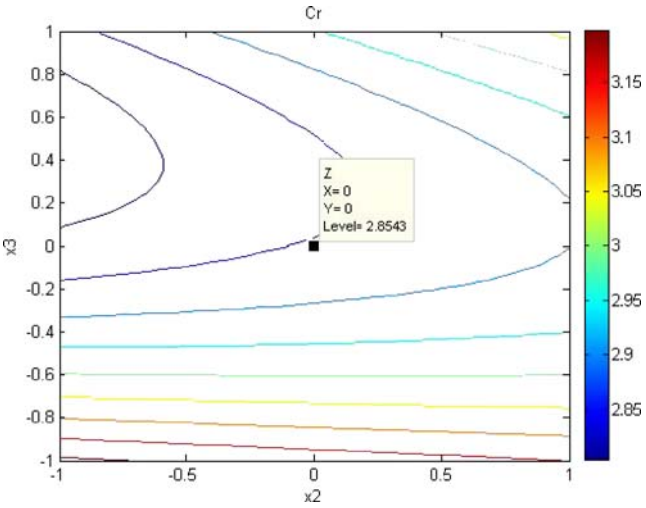

Fig. 6 Contour of RSM on Cr ($x_1 = -1$)

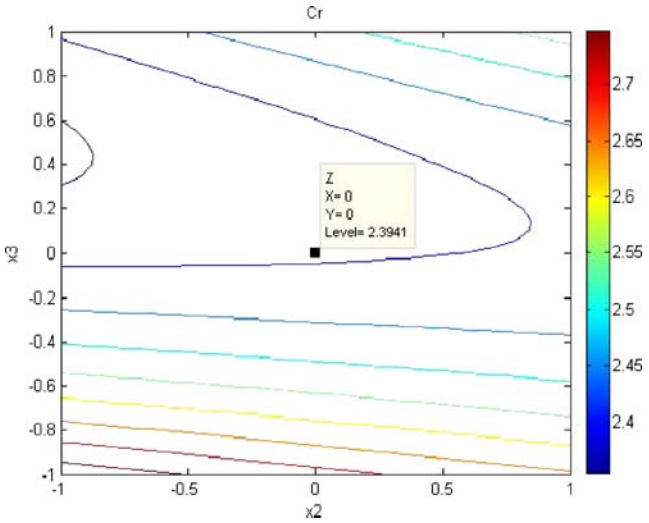

Fig. 7 Contour of RSM on Cr ($x_1 = 1$)

5.2 Building RSM model

Through the experiments mentioned above, the two order polynomial $f(x)$ is approximate by the design parameters (x_1, x_2, x_3). In term of Eq. (9), the $\widehat{\alpha}$ can be obtained by the least square method. The final functions of response surface model are listed as follows. The second-order polynomials of cooling effect is

$$\begin{aligned} c_r = {} & 2.7134 - 0.2301x_1 + 0.0256x_2 - 0.1822x_3 \\ & + 0.1151x_1^2 + 0.0027x_2^2 + 0.2074x_3^2 \\ & - 0.0168x_1x_2 + 0.0667x_1x_3 + 0.0725x_2x_3 \end{aligned} \tag{14}$$

5.3 Variance analysis of RSM

In order to verify whether the obtained second-order polynomials are appropriate or not, perform variance analysis and F-ratio test on them. Refer to probability statistics, $F=S_R/S_e$ is the F-distribution of first and second order of freedom, where

$$S_R = \sum_{j=1}^{k} \left(\widehat{y}_j - \overline{y}\right)^2 \tag{15}$$

$$S_e = \sum_{j=1}^{k} \left(y_j - \widehat{y}_j\right)^2 \tag{16}$$

So, when the conspicuous level α is specified, the critical value $F(f_R, f_e, \alpha)$ that satisfies the following equation can be looked up from F table.

$$P\{F > F(f_R, f_e, \alpha)\} = \alpha \tag{17}$$

If $F > F(f_R, f_e, \alpha)$, then consider the second-order polynomial is considered as a valuable model at α level. After calculation of F-ratio of cooling effect, we obtain F=54.6>F (9, 5, 0.01)=10.2. It shows that the polynomial of cooling rate is highly dramatic.

The F-ratio test shows that it is valuable for the corresponding problems. They can be used to analyze the relation between analysis objectives and design variables.

6 Analyzing and optimizing

6.1 RSM analyzing

According to the Eq. (14), we can obtain the 3D surface in coordinate reference when one of the variables is set to a constant. Figures 4 and 5 are the response surfaces of cooling rate when the design parameter x_1 is equal to -1 and 1. As shown in the two figures, the change about x_2 (pipe height) has no much effect on the cooling rate and the cooling rate can get the minimum when x_3 is equal to

Table 5 The best ten solutions of optimization results

No.	Factors			Design variables			Objective	Cooling rate
	x_1	x_2	x_3	v	h	D	f	c_r
1	0.8845	-1	0.515	14.34	1.0	4.32	0.4273	2.340276
2	0.885	-1	0.520	14.34	1.0	4.34	0.4273	2.340276
3	0.911	-1	0.520	14.49	1.0	4.34	0.4273	2.340276
4	0.838	-1	0.519	14.07	1.0	4.34	0.4273	2.340276
5	0.838	-1	0.519	14.07	1.0	4.34	0.4273	2.340276
6	0.838	-1	0.505	14.07	1.0	4.31	0.4273	2.340276
7	0.955	-1	0.510	14.74	1.0	4.32	0.4272	2.340824
8	0.955	-1	0.729	14.74	1.0	4.80	0.4260	2.347418
9	0.905	-0.607	0.440	14.46	2.4	4.17	0.4244	2.356268
10	0.955	-0.771	0.729	14.74	1.8	4.80	0.4236	2.360718

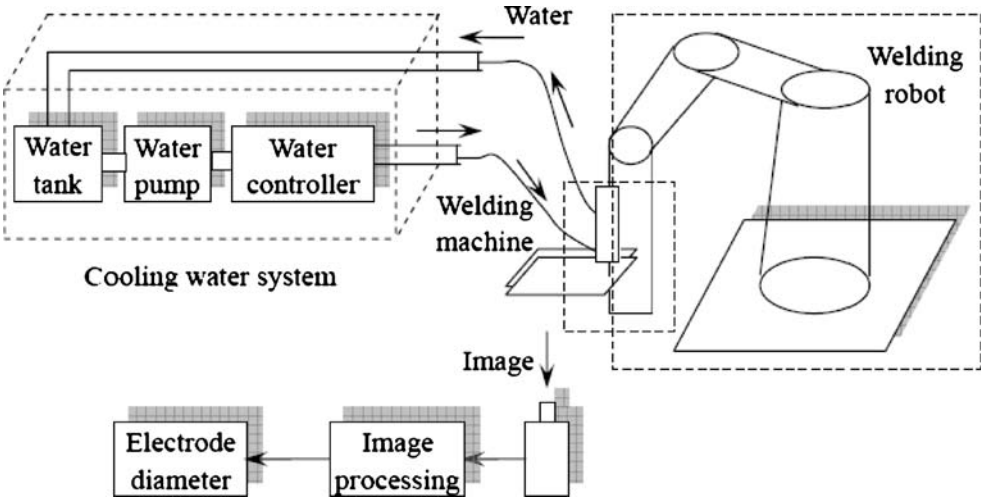

Fig. 8 Principle of the experiments

the value in [0, 1]. It means that the pipe diameter is in [3.2, 5.4].

Figures 6 and 7 are the contours of cooling rate when the design parameter x_1 is equal to -1 and 1. We can know from the figures that the cooling rates are 2.8543 and 2.3942 under the same structure configuration (x_2=0, x_3=0) when the water velocity gets the minimum and maximu,m respectively. When x_2 gets the value in [-1, 0.2] and x_3 in [0.3, 0.6], the cooling rate can get the minimum.

6.2 Optimizing design

Generally, the optimal results often locate in the area of the stationary point of response surface. To find the global optimal design parameters, further analysis will be performed to determine the location and the nature of the stationary point. In this study, GA method is utilized to find the optimizing parameters in the region of design variable. The fitness function is defined as:

$$f(v,h,D) = 1/c_r \tag{18}$$

According to the region of design variables, appropriate bit numbers are distributed to them and all of the three design variables are united into a binary character string with 18 bits as the chromosome. the GA optimization program complies, including the gene selection, gene copy, gene aberrance functions. The best ten solutions of optimization results are shown in Table 5.

7 Experiments validation

7.1 Cooling effect and electrode diameter

In continuous welding process, electrode wear occurs under periodic high temperature and high pressure. The present solution for this is by increasing of the diameter size. Electrode cooling is one of the important factors influencing electrode wear. The better the cooling effect is, the less the wear is and the smaller the diameter is. The cooling effect has an indirect connection with the electrode diameter. Therefore, experiments on electrode diameter are carried out to validate the optimal results.

7.2 Experiment principle

The experiment consists of two parts. One is the spot welding part, and another is the image collecting and processing part. As shown in Fig. 8, the spot welding part includes welding robot, server gun, control system and cooling system. Electrode is assembled on the arm of server gun, which is fixed on the welding robot. Cooling water is continuously supplied to cool the electrode. The image collecting and processing test initiates after the spot welding test. The carbon papers with electrode diameter

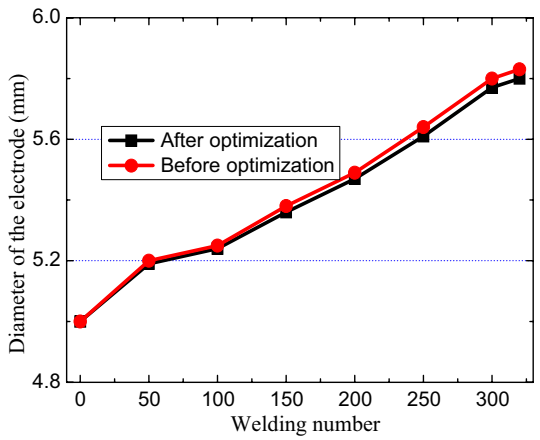

Fig. 9 Diameter change of the electrode before and after parameter optimization

image are collected by using digital camera. Finally, based on image processing method, experiment results of the electrode diameter under different cooling parameters are obtained.

7.3 Experiment results

According to above optimal results, a new cooling tube with a diameter of 4.32 mm has been employed, and its height has been changed from 3 mm to 1 mm. To avoid the interference from electrode pitting or other factors, only 320 continuous spot welding tests are performed with the old parameters and new after-optimization parameters, respectively. The results of different electrode diameters are shown in Fig. 9. It can be known that diameter size is reduced from 5.83 mm to 5.8 mm after the optimization, thus decreasing by 0.03 mm, while keeping the same cooling efficiency. It proves that the cooling effect has been improved and the electrode wear speed has becomes slower due to the parameter change. It is also known that the effect of the electrode diameter change is not obvious enough at the first 50 to 100 welds when the cooling effect improvement has not increased rapidly. As spot welding cycles later increase, the effect becomes more and more obvious and the advantages of electrode diameter optimization become more prominent.

8 Conclusion

This paper illustrates an experimental modeling approach for optimal cooling system parameters of the spot welding electrode. It discusses the approach from several points of view:

(1) The cooling model is established by finite element simulation. It performs flow and thermal analysis using various cooling system parameters.
(2) By response surface and experiment design method, the relationship between cooling rate and system parameters has been modeled, which can also been applied to other similar problem solving tasks.
(3) Subsequently, we adopt the response surface model to optimize system parameters by the GA method. The optimized results also show that proper arrangement of structure parameters can make obvious improvements of the cooling effect.
(4) Lastly, experiments are carried out to validate the optimal results by measuring the electrode diameter.

Acknowledgements This project is supported by Natural Science Foundation National of China numbered with 50575140 and 50605048.

References

1. Zhang XQ, Chen GL, Zhang YS (2008) Characteristics of electrode wears in resistance spot welding dual-phase steels. Mater Des 29(1):279–283 DOI 10.1016/j.matdes.2006.10.025
2. Rashid M, Fukumoto S, Medley JB (2007) Influence of lubricants on electrode life in resistance spot welding of aluminum alloys. Weld J (Miami, Florida) 86(3):62–70
3. Zhang XQ, Chen GL, Zhang YS (2006). On-line evaluation of electrode wear by servo gun in resistance spot welding. Int J Adv Manuf Technol, DOI 10.1007/s00170-006-0885-8
4. Wei L (2005) Modeling and on-line estimation of electrode wear in resistance spot welding. J Manuf Sci Eng 127(11):709–717
5. Kim E, Eagar TW (1998) Transient thermal behavior in resistance spot welding. Proceedings, Sheet Metal Welding Conference 2 (AWS-Detroit Section, Southfield, MI). Oct. Paper 2
6. Hensel FR, Larson EI, Holt EF (1941) Thermal gradients in spot welding electrodes. Weld J :850–856, Dec
7. Hirsch R (1996) Influence of water temperature and flow on electrode life. Proceedings, Sheet Metal Welding Conference 7 (AWS-Detroit Section, Troy, MI). Oct. Paper E3
8. IIW Working Group (1972) Welding of coated sheets, recommended practice for spot-welding zinc-coated steel sheets. Welding in the World 10(3/4)
9. Hensel FR, Larson EI, Holt EF (1942) Refrigerant-cooled spot-welding electrodes. Weld J Res Suppl 12:583–597
10. Lavery RC, Williams NT (1969) Resistance spot welding electrode wear on galvannealed steels. Metal Constr British Weld J 2:231–238
11. Yeung KS, Thornton PH (1999) Transient thermal analysis of spot welding electrodes. Weld J (Miami, Florida) 78(1):1–6
12. Davis LD (1991) Handbook of generic algorithms. Van Nostrand Reinhold, New York
13. Lin JC (2003) The Optimal Design of a Cooling System for a Die-Casting Die With a Free Form Surface. Adv Manuf Technol 21:612–619
14. Beal VE, Erasenthiran P, Hopkinson N, Dickens P, Ahrens CH (2006) Optimisation of processing parameters in laser fused H13/Cu materials using response surface method (RSM). J Mater Process Technol 174(1–3):145–154
15. Thornton PH, Krause AR, Davies RG (1995) Spot weld brazing of aluminum alloys. Proc. Int. Symp. Met. Adv. Vancouver, BC, Light Metals Industries, CIM, pp 217–228